ELSEVIER

NeuroImage

www.elsevier.com/locate/ynimg
NeuroImage 24 (2005) 678–691

Automatic analysis of cerebral asymmetry: an exploratory study of the relationship between brain torque and planum temporale asymmetry

Thomas R. Barrick,[a] Clare E. Mackay,[b] Sylvain Prima,[c] Frederik Maes,[d] Dirk Vandermeulen,[d] Timothy J. Crow,[b] and Neil Roberts,[a,*]

[a]*Magnetic Resonance and Image Analysis Research Centre (MARIARC), Pembroke Place, University of Liverpool, Liverpool L69 3BX, UK*
[b]*University Department of Psychiatry and POWIC, The Warneford Hospital, Headington, Oxford OX3 7JX, UK*
[c]*IRISA, Equipe VISAGES, Rennes, France*
[d]*Medical Image Computing, ESAT-PSI, Department of Electrical Engineering, K.U. Leuven, Belgium*

Received 20 March 2004; revised 28 July 2004; accepted 7 September 2004

Leftward occipital and rightward frontal lobe asymmetry (brain torque) and leftward planum temporale asymmetry have been consistently reported in postmortem and in vivo neuroimaging studies of the human brain. Here automatic image analysis techniques are applied to quantify global and local asymmetries, and investigate the relationship between brain torque and planum temporale asymmetries on T1-weighted magnetic resonance (MR) images of 30 right-handed young healthy subjects (15 male, 15 female). Previously described automatic cerebral hemisphere extraction and 3D inter-hemispheric reflection-based methods for studying brain asymmetry are applied with a new technique, LowD (Low Dimension), which enables automatic quantification of brain torque. LowD integrates extracted left and right cerebral hemispheres in columns orthogonal to the midsagittal plane (2D column maps), and subsequently integrates slices along the brain's anterior–posterior axis (1D slice profiles). A torque index defined as the magnitude of occipital and frontal lobe asymmetry is computed allowing exploratory investigation of relationships between this global asymmetry and local asymmetries found in the planum temporale. LowD detected significant torque in the 30 subjects with occipital and frontal components found to be highly correlated ($P < 0.02$). Significant leftward planum temporale asymmetry was detected ($P < 0.05$), and the torque index correlated with planum temporale asymmetry ($P < 0.001$). However, torque and total brain volume were not correlated. Therefore, although components of cerebral asymmetry may be related, their magnitude is not influenced by total hemisphere volume. LowD provides increased sensitivity for detection and quantification of brain torque on an individual subject basis, and future studies will apply these techniques to investigate the relationship between cerebral asymmetry and functional laterality.

Keywords: Automatic image analysis; Cerebral asymmetry; MRI

Introduction

Overview

Broca (1861) identified a major functional asymmetry in the human brain whereby for the majority of people speech production is linked preferentially to the left hemisphere. Lesion studies and, more recently, functional neuroimaging studies have established hemispheric specificity for a range of language, motor, and spatial tasks (e.g., Davidson and Hugdahl, 1995; Geschwind and Galaburda, 1985; Milner, 1971), but their relationship to underlying anatomy remains relatively poorly understood. Although the cerebral hemispheres are approximately equal in volume, weight, and density (e.g., Bastian, 1866; Braune, 1891), global and local structural asymmetries have been consistently reported. In particular, brain torque is a global asymmetry of hemispheric volume distribution such that the occipital and frontal lobes are leftwardly and rightwardly asymmetric, respectively. In addition, a region of the superior temporal lobe including the planum temporale has been consistently reported to be leftwardly asymmetric in volume, and this asymmetry has been related to language dominance (Geschwind and Levitsky, 1968). Thus far, anatomical studies quantifying torque (e.g., Bear et al., 1986) and planum temporale asymmetries (e.g., Geschwind and Levitsky, 1991) have been generally reliant on manual measurement, and to our knowledge, no previous study has specifically investigated the relationship

* Corresponding author. Magnetic Resonance and Image Analysis Research Centre (MARIARC), University of Liverpool, PO Box 147, Liverpool L69 3BX, UK. Fax: +44 151 794 5635.
E-mail address: neil@liverpool.ac.uk (N. Roberts).
Available online on ScienceDirect (www.sciencedirect.com).

1053-8119/$ - see front matter © 2004 Elsevier Inc. All rights reserved.
doi:10.1016/j.neuroimage.2004.09.003

between these global and local asymmetries, the existence of which might help elucidate the anatomical basis for development of functional laterality. Here we investigate the relationship between torque and planum temporale asymmetry by application of novel image analysis techniques designed to automatically quantify global and local brain asymmetry.

History of asymmetry measurement

Global asymmetry was first observed on postmortem specimens by Cunningham (1892) and was described as a greater volume of the left than the right occipital lobe. Further asymmetries were reported by Elliot-Smith (1907) as "unequal development of the frontal association areas" and "greater extent of the lateral part of left visual cortex". These global asymmetries were quantified in vivo on CT scans using width caliper measurements (LeMay, 1976, 1977; LeMay and Kido, 1978; Pieniadz and Naeser, 1984), and later by application of the same width measurement techniques to magnetic resonance (MR) images (Kertesz et al., 1990) and are referred to as brain torque. Cerebral width measurements have consistently revealed brain torque, but such techniques only provide a measurement at a single location that is highly dependent on subjective errors from slice positioning and landmark identification. More recently, volumetric torque has been described by manual outlining of lobar volumes by Bilder et al. (1999) on MR images. However, these planimetry methods are manually intensive and rely on subjective boundary identification.

Perisylvian asymmetries have also been described for over a century. The earliest reports indicated that the Sylvian fissure is both longer (e.g., Eberstaller, 1884; Rubens et al., 1976) and lower (Cunningham, 1892) in the left than the right. Contained within the Sylvian fissure on the superior surface of the temporal lobe is the planum temporale that has been reported to have a larger volume on the left than the right in postmortem (Geschwind and Levitsky, 1991; Pfeiffer, 1936) and MR imaging studies (Kulnych et al., 1994; Steinmetz, 1996). The association between leftward asymmetry of the planum temporale and left hemisphere 'dominance' for language functions was initially proposed by Geschwind and Levitsky (1968) and is supported by reports of reduced morphological asymmetry in patients with language disorders including dyslexia (e.g., Rumsey et al., 1986) and schizophrenia (e.g., Barta et al., 1997). In addition, planum temporale asymmetry has been related to handedness (Habib et al., 1995), with right-handers reported to have greater morphological asymmetry than left-handers (Steinmetz, 1996). However, not all studies have found significant asymmetry of the planum temporale volume (see Westbury et al., 1999), possibly due to difficulties in identification of the structure's superior and inferior boundaries on MR images. Here we will describe the use of new techniques that enable automatic extraction of the asymmetric region of the superior temporal gyrus without the need for subjective boundary identification.

Existing methods

The recent development of methods for intersubject registration and automatic segmentation of grey and white matter on high-resolution MR images has enabled group differences in brain structure to be investigated on a voxel-by-voxel basis (e.g., Ashburner and Friston, 2000). This methodology, known as voxel-based morphometry (VBM), has been applied to investigate cerebral asymmetry using reflection (Good et al., 2001; Watkins et al., 2001)- and deformation (Thirion et al., 2001)-based image registration techniques. Using VBM, Watkins et al. (2001) compared grey matter probability densities in left and right hemisphere voxels after normalizing (using a nine-parameter affine transformation) each image to standard space (Talairach and Tournoux, 1988) prior to reflection about the interhemispheric plane. Good et al. (2001) used a 12-parameter affine transformation and nonlinear basis functions, allowing modulation of tissue concentrations by the Jacobian determinant to preserve volumetric information. Results found by application of these techniques are interpreted as revealing either interhemispheric differences in tissue density (Watkins et al., 2001) or interhemispheric differences in tissue volume (Good et al., 2001), respectively. Thirion et al. (2001) described an alternative approach whereby volume differences between homologous structures in opposite cerebral hemispheres were quantified by application of an algorithm (Thirion, 1998) to nonrigidly co-register (deform) the left and right cerebral hemispheres with each other for each individual subject. From the corresponding interhemispheric vector deformation fields relative volume differences between homologous brain regions in the opposite hemispheres were computed. Specifically, the VBM techniques reveal reflection asymmetries that may either be due to regional structural displacement or tissue concentration/volume differences between the cerebral hemispheres, whereas the deformation techniques (Thirion et al., 2001) reveal only regional volume differences. Application of reflection and deformation asymmetry voxel-based analysis techniques has consistently revealed global torque and leftward planum temporale asymmetries. In the present study, we extend the reflection method to quantify brain torque and planum temporale asymmetry by extraction and integration of data for regions of interest (ROI).

LowD

Although brain torque has been visualized using 3D techniques such as those described above, it cannot be quantified without volume integration. We have developed a new method whereby grey and white matter voxels are integrated in cerebral hemispheres automatically extracted using the method of Maes et al. (1999). Integration is performed in columns perpendicular to the interhemispheric plane, reducing the data dimensionality to 2D. This generates an array of pixels in the sagittal plane representing column map volume asymmetry. Integration of column maps in coronal slices along the anterior posterior axis further reduces the data dimensionality to 1D and generates a profile of slice volume asymmetry. Reduction in dimensionality of the data gives the technique its name, LowD (Low Dimension). Column maps and slice profiles are output in standard space for groupwise statistical analysis of the partial dependence of volume asymmetries. In addition, column maps were integrated for anatomically defined regions to determine approximate lobe volume asymmetries. In particular, measurement of lobe asymmetry allows quantification of torque volume by summation of the magnitude of the occipital and frontal lobe asymmetries.

Objectives

The aim of the present study is to apply automatic image analysis techniques for identification and quantification of cerebral asymmetry for 15 male and 15 female healthy young right-handed subjects. The objectives are 2-fold: firstly, to establish techniques

for quantification of global and local asymmetry; and secondly, to investigate the relationship between brain torque and planum temporale asymmetry. In particular, global asymmetries of whole hemisphere grey, white, and total matter compartment volumes, column map, slice profile, and lobe volumes for male and female subjects are compared with local asymmetries determined from the reflection analysis. In addition, we present an exploratory investigation of sex differences in cerebral asymmetry.

Methods

Subjects and image acquisition parameters

MR images were acquired for 30 young, healthy subjects (15 males, mean age = 28.7, 15 females, mean age = 28.9). All subjects were right-handed and signed written informed consent of their willingness to participate in this study. For each subject, a 3D T1-weighted SPGR image comprising 124 contiguous coronal slices (TE = 9 ms, TR = 34 ms, NEX = 1, flip angle = 30°, 256 × 192 matrix, 20 cm field of view, thickness = 1.6 mm) was acquired using a 1.5-T SIGNA (G.E., Milwaukee, USA) whole body MR imaging system.

Image analysis

Data were analyzed on a SPARC Ultra 10 workstation (Sun Microsystems, Mountain View, CA) using SPM99 (Wellcome Department of Cognitive Neurology, Institute of Neurology, London), MATLAB 5.3 (The Math Works, Natick, MA), KUL (Katholieke Universiteit, Leuven, Belgium, including MIRIT: Multimodality Image Registration Using Information Theory, Maes et al., 1997), and LowD (in-house software, MARIARC, University of Liverpool, UK). Statistical analyses were performed using SPM99 and Statistical Package for Social Sciences (SPSS). Images were displayed using mri3dX (http://www.aston.ac.uk/lhs/staff/singhkd/mri3dX/index.html).

Image preprocessing

The following sections describe the methodology applied for the reflection and LowD asymmetry analyses. All preprocessing steps were performed in SPM99. In particular, each T1-weighted data set (referred to as being in acquired space) was normalized to a symmetric version of the MNI305 template (referred to as standard space) (Evans et al., 1993) by application of a 12-parameter affine transformation (Friston et al., 1995). Images were then segmented into grey and white matter concentration maps, incorporating a correction for image intensity nonuniformity (Ashburner and Friston, 2000; Ashburner et al., 1997). For each T1-weighted data set, these steps provided intensity nonuniformity corrected grey and white matter tissue segmentations in standard (for the reflection asymmetry analysis) and acquired space (for the LowD asymmetry analysis), and a 4 × 4 affine transformation matrix mapping the acquired T1-weighted image to standard space.

Reflection asymmetry analysis

For each subject, the normalized intensity nonuniformity corrected grey and white matter segmentation images were individually reflected about the midsagittal plane ($x = 0$) in standard space. Voxelwise asymmetry measures were calculated by subtraction of the reflected image from the unreflected image. These reflection-based asymmetry measures correspond to difference in tissue probability between the two hemispheres, such that a positive-valued voxel has a greater tissue concentration in the ipsilateral with respect to the contralateral hemisphere.

The reflection method applied in the present study and by Good et al. (2001) differs from Watkins et al. (2001) by application of a 12-parameter affine image normalization rather than a nine-parameter transformation. Twelve-parameter transformations include skew in addition to the nine parameters of translation, rotation, and scale. Skew parameters reduce the effect of greater extension of the occipital and frontal poles (petalias) in the left and right hemispheres, respectively. Chance et al. (2004) report that brain torque and petalia extension are separate variables so reduction of petalia extension should provide more accurate quantification of brain torque. A further difference between previous applications of the reflection asymmetry technique is such that we and Good et al. (2001) used an interleaved algorithm for tissue segmentation and intensity nonuniformity correction (Ashburner and Friston, 2000; Ashburner et al., 1997), whereas Watkins et al. (2001) performed separate intensity nonuniformity (Sled et al., 1998) and tissue segmentations based on T1, T2, and PD images (Zijdenbos et al., 1998).

LowD

A three-step method was used to generate 2D column map and 1D slice profile asymmetry maps:

(1) The cerebral hemispheres were extracted from the acquired 3D images using the technique of Maes et al. (1999). This method registers a template image (defined by a single subject from the Internet Brain Segmentation Repository (Worth, http://neurowww.mgh.harvard.edu/cma/ibsr) for whom the cerebral hemispheres superior to the tectum have been manually segmented) to each study image using a 12-arameter affine transformation (MIRIT: Maes et al., 1997) followed by a nonrigid deformation (Thirion, 1998). These registration parameters were then applied to deform a binary mask of the template supratentorial cerebral hemispheres to the study image. By overlaying this deformed mask on the grey and white matter segmentations in acquired space, these compartments were extracted for the left and right hemispheres. Morphological operations of erosion, largest component extraction, and dilation were then used to remove regions of dura that still remained after hemisphere extraction. Cerebral hemisphere volumes for grey, white, and total matter were calculated by integration of the parcellated tissue segmentation images, and volumetric asymmetry was computed by subtraction of the left hemisphere volume from the right.

(2) 2D column map and 1D slice profile volumes were obtained as illustrated in Fig. 1. For 2D column maps, the inverse affine transformation of each image into standard space was used to transform a 2D array of 242 × 174 0.781^2 mm pixels in the midsagittal plane of standard space to the interhemispheric plane in acquired space. This 2D array representing grey, white, and total matter volumes was calculated as the summation of interpolated voxel volumes for the left and right cerebral hemispheres in columns perpendicular to the interhemispheric plane (Fig. 1, blue arrows). For 1D slice

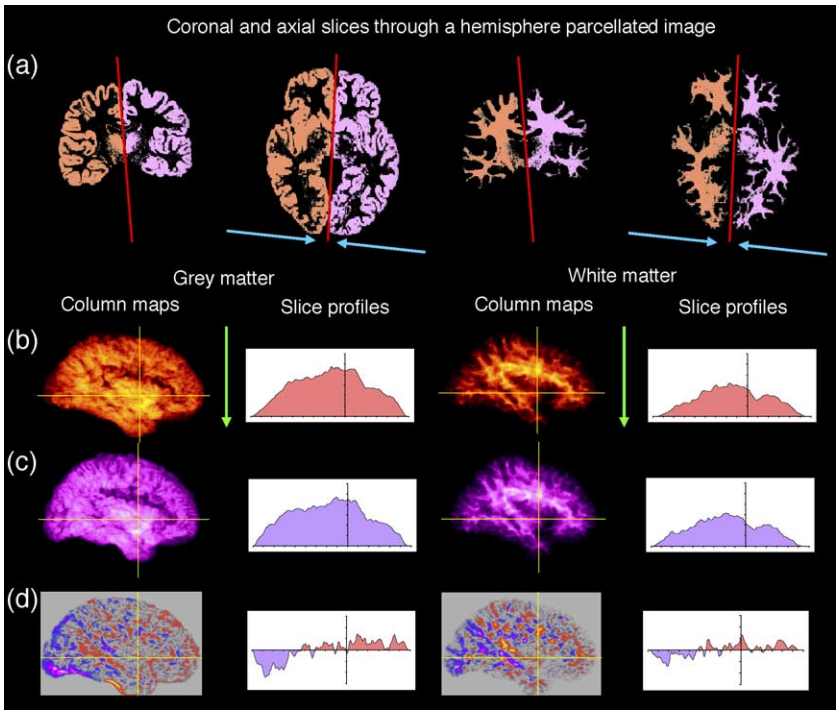

Fig. 1. Method for computation of grey and white matter column map and slice profile images. (Row a) illustrates grey and white matter tissue concentration images for axial and coronal slices of a single subject in acquired space. These images are overlain with the interhemispheric symmetry plane indicated by the red line. The left and right cerebral hemispheres are colored purple and orange, respectively. By integration along the blue arrows (in row a) perpendicular to the symmetry plane, volumetric column maps are computed for the right (row b) and left (row c) hemispheres and are output in standard space. Integration of the column maps along the direction of the green arrows generates coronal slice profile graphs for the right (row b) and left (row c) hemispheres. Asymmetry images computed by right hemisphere–left hemisphere are illustrated for column map and slice profiles (row d) with hot and cold colors representing rightward and leftward volume asymmetries, respectively.

profiles, the superior–inferior dimension of the 2D column map in standard space was integrated to give an anterior–posterior profile corresponding to two hundred forty-two 0.781-mm-thick slices (Fig. 1, green arrows). Appropriate voxel scalings were applied so that the column map and slice profile hemisphere volumes in standard space are equivalent to the hemispheric volumes in acquired space.

(3) Asymmetry images for grey, white, and total matter 2D column and 1D slice profile data were calculated on a pixel-by-pixel and slice-by-slice bases by subtraction of volumes in the left hemisphere column, or slice, from the right hemisphere (see Fig. 1).

Volumes of grey, white, and total matter for individual lobes were also computed. In particular, 2D lobe masks were generated using anatomical criteria defined by projecting lobe boundaries drawn on a rendered 3D image in standard space to the sagittal plane (Fig. 5a). Column maps were then integrated under the mask to determine approximate volumes for frontal, temporal, parietal, and occipital lobes. Asymmetry measures were calculated by subtraction of the left lobe volume from the right. A global brain torque index was quantified by addition of the modulus of frontal and occipital lobe volume asymmetry.

Prestatistical processing

Prior to statistical analysis the 3D reflection images were smoothed using a 10-mm FWHM isotropic Gaussian filter as described by Watkins et al. (2001). Column maps and slice profiles were smoothed by 6- and 3-mm FWHM isotropic Gaussian filters, respectively. Selection of filter sizes was performed empirically and takes into account increases in image smoothness when data are integrated from 3D to 2D to 1D. In particular, the selection of filter sizes was chosen to provide similar smoothness of the residual images (defined by the RESEL (resolution element) count) across all asymmetry analyses. Smoothing was applied to the 3D, 2D, and 1D asymmetry images in contrast to Watkins et al. (2001) and Good et al. (2001) who smoothed tissue concentration images prior to computation of reflection asymmetry images. However, whether smoothing is performed before or after asymmetry quantification will not have an effect on the results of subsequent statistical analyses because computation of reflection asymmetry by voxel-wise subtraction of left and right hemisphere data is a linear process.

To ensure statistical analysis referred only to voxels of high tissue concentration across all individuals, a binary mask was constructed for each asymmetry analysis. For the 3D reflection analysis, this binary mask was formed by determining the inclusion set of all voxels surviving a proportional threshold of 80% in each of the smoothed reflected and unreflected images (i.e., the standard VBM preprocessing step). Due to integration, voxels close to the periphery of the left and right hemispheres in 2D column maps and 1D slice profiles have proportionally lower volumes than those in the center. To generate whole brain masks, lower proportional thresholds of 40% and 5% were qualitatively selected for the 2D- and 1D-smoothed left and right hemisphere data, respectively, on the basis that they restricted column map and slice profile investigations to similar brain regions to those included in the reflection analysis. Effectively, this step removed pixels in a

boundary annulus from the column map, and the anterior–posterior cerebral limits from the slice profile images.

Statistical analysis

ANOVA

Reflection and LowD column map and slice profile techniques produce output asymmetry images for each subject in standard space. For each technique, statistical investigations of average and sexually dimorphic asymmetry were performed using an ANOVA design in SPM99 incorporating appropriate corrections for multiple comparisons using random Gaussian fields (Worsley et al., 1996). Asymmetry images were analyzed as the dependent variable in a two-group design matrix that included a between subject factor of sex (male, female). Results were considered significant at $P < 0.05$ corrected for peak height over the whole volume analyzed.

Scalar volumetric data were analyzed in SPSS to test for main effects of sex and asymmetry in hemisphere and lobe volume using a repeated measures MANOVA design. The between subject factor was sex (male, female) and within-subject factor was asymmetry (left, right). For lobe volumes, an additional within-subject factor of lobe (frontal, temporal, parietal, occipital) was included.

Regression

The relationship between asymmetry measures and total brain volume was investigated using linear regression for all asymmetry analysis techniques. For reflection, column map, and slice profile asymmetry images, this was achieved by investigating the relationship between asymmetry and total compartment volume covariates. For whole hemisphere and lobar asymmetry, the relationships were investigated between asymmetry and brain volumes computed by addition of the left and right hemisphere total matter volumes output from the hemisphere extraction technique. Linear regression for reflection and LowD methods was performed using SPM99, and appropriate corrections for random Gaussian fields were applied (Worsley et al., 1996). Results were considered significant at $P < 0.05$ corrected for peak height over the whole volume analyzed. Linear regressions for whole hemisphere and lobar asymmetry analyses were performed using Pearson's product moment statistic in SPSS. All of the above analyses were performed for the male and female groups, separately and combined.

Post hoc analysis was performed to investigate the relationship between planum temporale asymmetry and grey matter torque volume. A region of interest (ROI) was defined for the reflection analysis as the region of significant average grey matter asymmetry located in the planum temporale (see Fig. 5b). For each subject, the average asymmetry measure was computed within the ROI. The relationship between planum temporale asymmetry and global grey matter torque volume was then investigated using Pearson's product moment statistic in SPSS.

Table 1
Descriptive statistics for grey, white, and total matter left and right hemisphere volumes in male and female subjects

Matter type	Population	Mean	Minimum	Maximum	Standard error
Grey (left)	Male	303.2	256.4	337.5	6.1
	Female	280.8	237.0	304.8	6.0
	Combined	292.0	237.0	337.5	4.7
Grey (right)	Male	302.3	254.5	336.6	6.2
	Female	283.5	237.8	310.3	6.1
	Combined	292.9	237.8	336.6	4.6
White (left)	Male	196.8	159.2	242.0	6.3
	Female	175.7	152.7	206.3	3.9
	Combined	186.2	152.7	242.0	4.1
White (right)	Male	198.6	159.3	246.2	6.5
	Female	177.0	154.2	208.3	3.8
	Combined	187.8	154.2	246.2	4.2
Total (left)	Male	500.0	415.5	568.8	10.6
	Female	456.5	404.1	511.1	7.2
	Combined	478.2	404.1	568.8	7.5
Total (right)	Male	500.9	416.2	571.9	10.6
	Female	460.5	410.8	508.3	7.1
	Combined	480.7	410.8	571.9	7.3
Grey asymmetry	Male	−0.83	−6.70	4.59	0.65
	Female	2.78	−4.88	10.18	0.86
	Combined	0.97	−6.70	10.18	0.63
White asymmetry	Male	1.79	−4.05	6.73	0.70
	Female	1.27	−2.36	6.11	0.59
	Combined	1.53	−4.05	6.73	0.45
Total asymmetry	Male	0.96	−5.24	5.58	0.80
	Female	4.05	−2.87	8.45	0.87
	Combined	2.50	−5.24	8.45	0.65
Grey/white ratio (left)	Male	1.55	1.18	1.78	0.04
	Female	1.61	1.18	1.92	0.05
	Combined	1.58	1.18	1.92	0.03
Grey/white ratio (right)	Male	1.54	1.13	1.81	0.04
	Female	1.61	1.17	1.91	0.05
	Combined	1.58	1.13	1.91	0.03

Results

Global asymmetry

Cerebral hemisphere volume

Mean left and right hemisphere volumes, hemisphere asymmetries for grey, white, and total matter, and grey/white matter ratios are presented in Table 1. For both sexes combined, mean rightward asymmetry was observed for all tissue types but was significant only in white (F = 11.1, [29:1], P = 0.002) and total matter (F = 18.0, [29:1], P < 0.001).

Total matter brain torque asymmetry

Results of cerebral hemisphere asymmetry analyses for the combined grey and white matter compartments are illustrated in Fig. 2 with corresponding voxel significances and locations presented in Table 2. In the following text and in Table 2, significant total matter column map asymmetries are coded CT.

Significant brain torque components were detected in column maps by leftward asymmetry in the occipital lobe (CT2) and rightward asymmetry in the frontal lobe (CT1), see Fig. 2c. In addition, significant leftward asymmetry was found in the posterior parietal (CT5, CT8) and temporal lobes (CT7), and significant rightward asymmetry in the parietal (CT4) and superior temporal lobe (CT3, CT6). Torque was also significant in 1D slice profiles (Fig. 2e). A large region of leftward asymmetry was found extending from the anterior occipital lobe boundary to the approximate occipital pole (y = −62 mm). Similarly, a large region of rightward asymmetry was revealed extending from the frontal pole to the anterior frontal lobe boundary (y = −25 mm). Furthermore, brain torque was detected by a significant asymmetry by lobe interaction (F = 32.0, [28:1] P < 0.001) such that occipital and frontal lobe volumes were larger in the left and right hemispheres, respectively.

Grey and white matter brain torque asymmetry

Results of cerebral hemisphere asymmetry analyses for the segmented grey and white matter compartments are illustrated in Figs. 3 and 4 with corresponding voxel significances and locations presented in Table 3. In the following text and Table 3, significant grey matter reflection-based and column map asymmetries are coded RG and CG, respectively, with white matter asymmetries coded RW and CW.

No significant brain torque was detected for reflection analyses of grey and white matter although nonsignificant trends for average leftward occipital and rightward frontal lobe asymmetry were observed (Figs. 3a and 4a). However, significant brain torque components were detected in column maps (Figs. 3h and 4h) as leftward asymmetry in the occipital lobe (CG1, CW2) and rightward asymmetry in the frontal lobe (CG2, CW4). A single exception to this pattern was a region of significant leftward asymmetry in posterior orbital prefrontal white matter (CW6). In addition to the brain torque components, several significant regions with opposite asymmetry in grey and white matter were identified in the perisylvian region of the inferior frontal and superior temporal lobes (grey matter: CG4, CG8, CG9; white matter: CW1, CW3, CW7). These are described in the local asymmetry section below. Torque was also detected in grey and white matter slice profile analyses as significant posterior leftward and anterior rightward asymmetry (Figs. 3h and 4h). In both the grey and white matter column map and slice profile analyses,

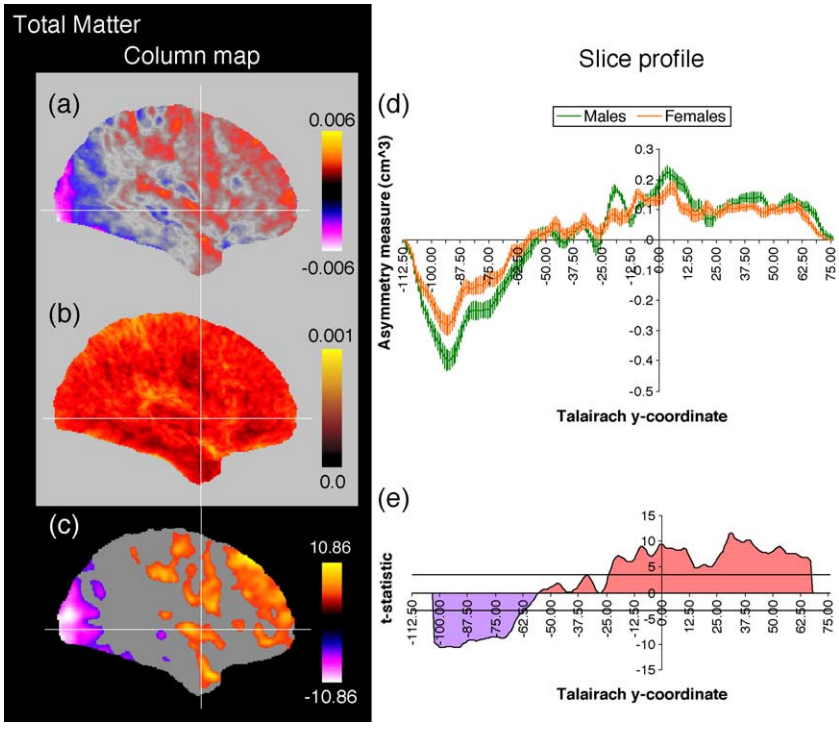

Fig. 2. Total matter asymmetry results. Average total matter column map asymmetry (a) and standard error (b) images are shown above significance maps of the t statistic (c). Average total matter slice profiles are illustrated for male (green) and female (orange) subjects with standard error bars marked (d) above a graph of the t statistic across the male and female subjects combined (e). The black horizontal lines above and below the x axis in graph (e) represent the t statistic threshold beyond which slice profile asymmetries are significant. Hot and cold colors represent rightward and leftward asymmetries in the column map and slice profile results.

Table 2
Regions of significant asymmetry revealed by the 2D total matter column map analysis

Code	*y*, *z* stereotactic coordinate	Cluster area (cm^2)	Asymmetry	Description
CT1	33, 49	15.11	R	Frontal lobe torque
	8, 17	7.01	R	(three clusters)
	27, 2	0.59	R	
CT2	−93, 10	9.78	L	Occipital lobe
	−52, −20	0.40	L	torque (three clusters)
	−79, 45	0.37	L	
CT3	7, −32	6.34	R	Anterior temporal lobe
CT4	−26, 37	5.19	R	Inferior parietal lobe
	−46, 54	0.43	R	(two clusters)
CT5	−70, 26	1.00	L	Posterior parietal lobe at posterior callosal boundary
CT6	−25, 10	0.49	R	Superior posterior temporal lobe (two clusters)
CT7	−27, −3	0.37	L	Posterior temporal lobe
CT8	−24, 21	0.13	L	Inferior posterior frontal lobe

brain torque components were more fragmented than those found by the total matter analysis. Brain torque was also detected by a significant asymmetry by lobe interaction such that occipital and frontal lobe volumes were larger in the left and right hemispheres, respectively, for both the grey and white matter compartments (grey matter: $F = 50.2$, [28:1] $P < 0.001$; white matter: $F = 6.5$, [28:1] $P = 0.017$).

Local asymmetry

Perisylvian asymmetry

Significant leftward asymmetry in the region of the planum temporale was detected by the grey matter reflection (RG4, Fig. 3c) and column map analyses (CG4, Fig. 3f). Further significant asymmetries were detected by column map analyses in the perisylvian region. In particular, rightward asymmetry in grey matter was found superior and inferior to the planum temporale along the superior temporal sulcus/middle temporal gyrus (CG8) and a section of the posterior inferior frontal gyrus (CG9). White matter asymmetries were in antiphase to the grey matter findings (Fig. 4f). In particular, rightward asymmetry was detected in the planum temporale region (CW1) with leftward asymmetry found superiorly in the posterior inferior frontal lobe (CW7) and inferiorly in white matter underlying the middle temporal gyrus (CW3). Several of these asymmetries were replicated by the reflection analysis: rightward grey matter superior temporal sulcus (RG12), rightward white matter below the superior temporal gyrus (RW8), and leftward white matter below the middle temporal gyrus (RW3). In Fig. 6, the significant antiphase grey and white matter column map asymmetries (Figs. 6a and 6b) are overlain on coronal slices of grey and white matter through the perisylvian region (Figs. 6c and 6d). Fig. 6 shows that the superior temporal lobe morphology differs between left and right hemispheres, with grey

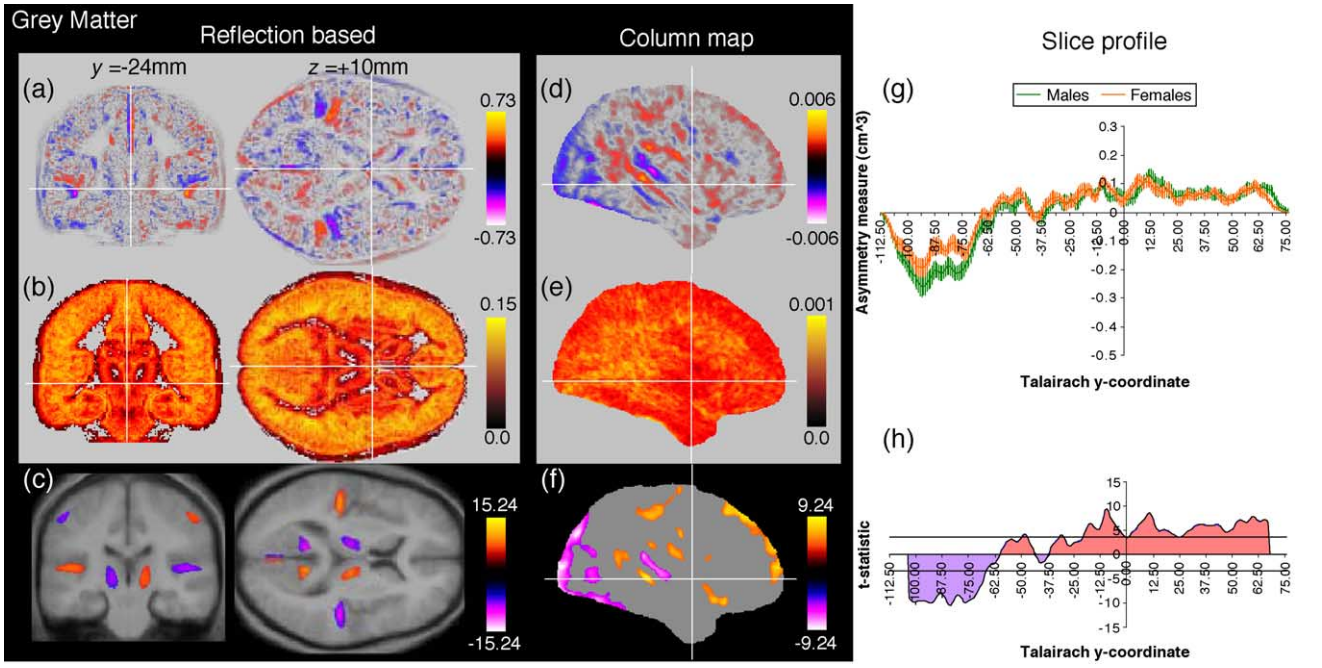

Fig. 3. Grey matter asymmetry results. Average grey matter asymmetry images (a and d) and standard error images (b and e) are shown above significance maps of the *t* statistic (c and f) for the reflection and column map analyses. Reflection asymmetry results are illustrated through coronal (Talairach slice $y = -24$ mm) and axial (Talairach slice $z = +10$ mm) slices in standard space with statistically significant results overlain on the mean T1-weighted image computed across all 30 subjects. All 3D images are displayed using the neurological convention. Average grey matter slice profiles are illustrated for male (green) and female (orange) subjects with standard error bars marked (g) above a graph of the *t* statistic across the male and female subjects combined (h). The black horizontal lines above and below the *x* axis in graph (h) represent the *t* statistic threshold beyond which slice profile asymmetries are significant. Hot and cold colors represent larger and smaller regions for the ipsilateral hemisphere in the reflection results and rightward and leftward asymmetries in the column map and slice profile results, respectively.

Table 3
Regions of significant grey matter asymmetry revealed by 3D reflection and 2D column map analyses

Code	*x*, *y*, *z* stereotactic coordinate	Cluster volume (cm^3)	Asymmetry	Description
3D grey matter reflection				
RG1	4, −63, 23	2.10	R	Cuneus
RG2	28, 23, −15	2.12	R	Orbital gyrus
RG3	8, −42, −24	2.06	R	Cerebellum
RG4	−46, −27, 12	1.87	L	Planum temporale
RG5	11, −16, 9	1.51	R	Thalamus
RG6	52, −18, 48	1.41	R	Inferior parietal
	54, −49, 35	0.16	R	lobe (four clusters)
	56, −26, 24	0.10	R	
	47, −56, 47	0.10	R	
RG7	1, −41, 44	0.47	R	Precuneus
RG8	−11, 8, 2	0.47	L	Caudate
RG9	−11, 37, −14	0.42	L	Rectal gyrus
RG10	1, −79, 11	0.29	R	Lingual gyrus
RG11	−26, −40, −38	0.24	L	Anterior cerebellum
RG12	49, −36, 7	0.22	R	Superior temporal sulcus
RG13	−49, −46, −22	0.22	L	Superior cerebellum
2D grey matter column map (y and z coordinates only, cluster area in cm^2)				
CG1	−98, 9	6.88	L	Occipital lobe
	−76, 5	1.18	L	torque (two clusters)
CG2	62, 9	4.34	R	Frontal
	−9, 33	0.32	R	lobe torque
	−9, 66	0.24	R	(four clusters)
	12, 16	0.12	R	
CG3	−32, 47	1.92	R	Inferior parietal lobule/Precuneus
CG4	−36, 17	1.67	L	Planum temporale
CG5	23, −16	1.32	R	Orbital gyrus
CG6	−55, 15	1.08	R	Cuneus
CG7	−14, 20	0.96	R	Thalamus
CG8	−34, 2	0.74	R	Superior temporal sulcus/Middle temporal gyrus
CG9	−30, 25	0.29	R	Posterior inferior frontal gyrus

matter more prominent in the left and white matter more prominent in the right.

Local asymmetry outside the perisylvian region

Outside the perisylvian region, several local grey and white matter reflection asymmetries were detected (see Tables 3 and 4). Grey matter results include rightward asymmetry of the cuneus (RG1), thalamus (RG4), and parietal grey matter (RG6) and leftward asymmetry of the caudate (RG8).

Relationship between global and local asymmetry

A significant positive correlation was found between leftward planum temporale asymmetry and torque index ($r = 0.632$, $P < 0.001$) (see Fig. 5d). Components of torque were related such that rightward frontal asymmetry was negatively correlated with leftward occipital asymmetry in the grey matter ($r = -0.64$, $P < 0.001$), white matter ($r = -0.73$, $P < 0.001$), and total matter ($r = -0.80$, $P < 0.001$) (Fig. 5c).

No significant correlations were found between total brain volume and asymmetry for voxelwise 3D reflection or pixelwise 2D column asymmetry measures. Also, no correlation was observed between brain size and lobe asymmetry or torque index. A significant correlation between asymmetry and total brain volume was revealed in 1D slice profiles for a single 3-pixel region of white matter ($t < -3.57$, min $t = -4.02$, [29:1], $P = 0.017$, y-coordinate range 22–24 mm) for the combined group of male and female subjects.

Sex differences

Mean cerebral hemisphere volumes were larger in males for all tissue types ($F > 4.6$, [29:1], $P < 0.05$) (Table 1). Significant sexual dimorphism was revealed in hemispheric volume for grey matter ($F = 11.2$, [29:1], $P = 0.002$) and total matter ($F = 11.2$, [29:1], $P = 0.002$). In particular, males exhibited a leftward and females a rightward asymmetry for grey matter and females exhibited greater rightward asymmetry than males for total matter. Greater variance was observed in white matter volumes for males relative to females, but this did not reach statistical significance (left: Levene's statistic = 2.7, [28:1], $P = 0.11$; right: Levene's statistic = 3.1, [28:1], $P = 0.09$).

A region of significant sexual dimorphism (Fig. 4g) revealed by analysis of white matter slice profiles was located posterior to the anterior commissure ($t > 3.57$, max $t = 4.01$, [28:1], $P = 0.018$, size = 4 pixels, y-coordinate range −16 to −19 mm). In this region, males had significantly increased rightward asymmetry relative to females. No other significant sex differences were found by reflection or LowD analyses although males tended to have increased leftward occipital asymmetry relative to females in total and grey matter (for total matter see Fig. 2d, posterior to $y = -57$ mm; for grey matter see Fig. 3g, posterior to $y = -61$ mm).

Discussion

We have described techniques for automatically quantifying global and local asymmetry and demonstrated a significant correlation between brain torque and leftward planum temporale asymmetry. Frontal and occipital components of torque were also highly correlated, but asymmetry measures did not correlate with total brain volume. Exploratory investigations of sex differences in cerebral asymmetry revealed a region of white matter posterior to the anterior commissure where significantly greater rightward asymmetry was found in males. Consideration of generic methodological issues of automatic segmentation and their effect on cerebral asymmetry analyses are discussed before consideration of the biological interpretation of the results.

Methodological considerations

Grey/white matter ratios found by the cerebral hemisphere extraction technique (mean = 1.6, see Table 1) were similar to those reported by Maes et al. (1999) but did not correspond with data from a postmortem study by Miller et al. (1980). Miller et al. (1980) reported a ratio of 1.3 at the age of 20, decreasing to 1.1 at the age of 50. Pre- and postmortem grey and white matters do not have the

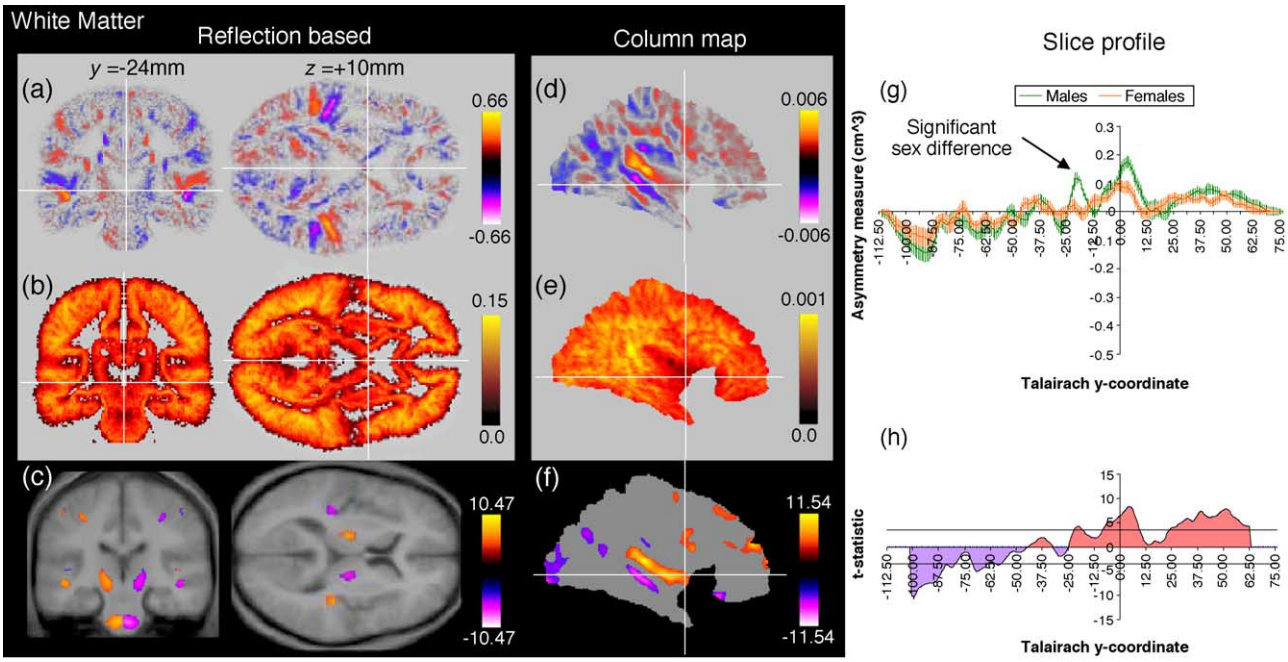

Fig. 4. White matter asymmetry results. Format is identical to that in Fig. 3.

same MR tissue characteristics (Blamire et al., 1999), partly due to the process of fixation (Garcia-Finana et al., 2003). The a priori grey and white matter tissue probability images used by the tissue segmentation algorithm (Ashburner et al., 1997) have a grey/white matter ratio of approximately 1.6 and may introduce a systematic bias. To improve tissue segmentation and more reliably label voxels at interfaces between tissue types (i.e., at partial volume boundaries), it may be necessary to acquire multimodal PD, T1-, and T2-weighted images and use tissue segmentation methods such as Zijdenbos et al. (1998), Van Leemput et al. (1999a,b), or Zhang et al. (2001). In particular, the methods of Zijdenbos et al. (1998) and Zhang et al. (2001) do not require a priori information in the form of initial tissue probability images.

Glicksohn and Myslobodsky (1993) showed that the symmetry plane of the brain is frequently non-coplanar to the interhemispheric fissure and deviates to the right in the occipital falx. The occipital falx offers different potential limitations to each automatic asymmetry quantification technique applied in the present study. Reflection-based asymmetry requires identification of the interhemispheric symmetry plane, and artefacts will arise where the falx curves in the occipital lobe. Cerebral hemisphere extraction is not dependent on the symmetry plane because voxel assignment to the left or right hemisphere is determined by nonrigid registration of an extracted template image to the subject image. However, integration of column maps perpendicular to the symmetry plane could potentially exaggerate leftward asymmetry in the occipital lobe because the falx, in general, deviates to the right in this region (Glicksohn and Myslobodsky, 1993). To improve the accuracy of reflection and column map quantification, the asymmetry measures could be computed perpendicular to multiple planes or perpendicular to a curved surface defining the interhemispheric fissure. However, such solutions would render reflection asymmetries difficult to interpret, and left and right column map and slice profile images would no longer represent actual brain volumes, and hence were not investigated in the present study.

Biological interpretation

Small but significant rightward asymmetry was detected in the cerebral hemisphere white and total matter volume. Previously, both leftward and rightward asymmetry in total hemisphere volumes have been reported for studies using postmortem (leftward: Aresu, 1914; rightward: Skullerud, 1985; Zilles et al., 1996); manual MRI measurement (leftward: Mackay et al., 1998; rightward: Mackay et al., 2000; Zilles et al., 1996); and automatic MRI measurement (leftward: Maes et al., 1999; Zilles et al., 1996; rightward: present study) techniques. These inconsistencies, as well as reports of no consistent asymmetry in weight or density (e.g., Bastian, 1866; Braune, 1891; Maes et al., 1999; Weil, 1929), lead us to conclude that the left and right cerebral hemispheres are essentially equal in volume, but that differences in methodology and/or cohort give rise to small differences between the hemispheres that reach statistical significance in some studies.

Consistent with postmortem analyses of skull shape (LeMay, 1976; 1977), postmortem brain widths (Pieniadz and Naeser, 1984; Weinberger et al., 1982), in vivo CT widths (Bear et al., 1986; Chui and Damasio, 1980; LeMay and Kido, 1978; Pieniadz and Naeser, 1984), MR widths (Kertesz et al., 1986; 1990), manual MR volumetry studies (Bilder et al., 1994, 1999; Falk et al., 1991; Steinmetz and Galaburda, 1991), and automatic MR reflection asymmetry studies (Good et al., 2001; Watkins et al., 2001), brain torque was detected in the present study. However, in contrast to the larger data sets of Watkins ($N = 142$) and Good ($N = 465$), significant brain torque was not detected by the reflection asymmetry technique, although trends toward mean leftward occipital and rightward frontal lobe asymmetry were observed. Significant brain torque was revealed by column map and slice profile techniques indicating that the LowD approach is more sensitive to detecting brain torque in small groups of subjects than voxelwise reflection asymmetry techniques. Consistent with previous reports (Bear et al., 1986; LeMay and Kido, 1978), no incidence of reversed torque (i.e.,

Table 4
Regions of significant white matter asymmetry revealed by 3D reflection and 2D column map analyses

Code	*x*, *y*, *z* stereotactic coordinate	Cluster volume (cm^3)	Asymmetry	Description
3D white matter reflection				
RW1	−15, −15, −5	3.17	L	Corticospinal tracts into internal capsules
RW2	−4, −25, −30	2.30	L	Brainstem
RW3	−48, −35, 5	0.75	L	White matter below the middle temporal gyrus
RW4	10, 37, −14	0.66	R	Anterior medial orbital prefrontal
RW5	−33, 31, −10	0.56	L	Anterior lateral orbital prefrontal
RW6	14, 8, 2	0.39	R	Anterior limb internal capsule
RW7	−16, −51, 20	0.34	L	Posterior callosal boundary
RW8	38, −29, 12	0.23	R	White matter below the superior temporal gyrus
RW9	18, −50, 36	0.15	R	Superior to posterior callosal boundary
RW10	−49, −10, −16	0.13	L	White matter below the inferior temporal gyrus
2D white matter column map (y and z coordinates only, cluster area in cm^2)				
CW1	−28, 9	4.22	R	Anterior temporal stem/ Anterior limb of internal capsule/White matter underlying superior temporal gyrus
CW2	−95, −4	2.04	L	Occipital lobe torque
CW3	−28, −3	1.37	L	Posterior temporal stem/ White matter underlying middle temporal gyrus
CW4	5, 19	1.04	R	Frontal lobe torque
	47, 22	0.96	R	
	21, 46	0.84	R	
	−6, 54	0.27	R	
	31, 21	0.26	R	
	56, 10	0.24	R	
CW5	−68, 29	0.72	L	Posterior parietal lobe at posterior callosal boundary (two clusters)
	−57, 18	0.42	L	
CW6	23, −13	0.35	L	Anterior lateral orbital prefrontal
CW7	−29, 24	0.18	L	Inferior posterior frontal lobe

leftward frontal and rightward occipital asymmetry) was found by volumetric analysis of these right-handed subjects, and a strong correlation was observed between frontal and occipital brain torque components (Bear et al., 1986).

Significant leftward asymmetry was revealed in the region of the planum temporale by reflection and column map analyses consistent with postmortem (Geschwind and Levitsky, 1968; Witelson and Kigar, 1992), MRI morphometry (Foundas et al., 1994, 1999; Kulnych et al., 1994; Steinmetz, 1996; Steinmetz et al., 1989), and MRI voxelwise reflection studies (Good et al., 2001; Watkins et al., 2001). Rightward asymmetry of the superior temporal sulcus was also revealed by both the reflection and column map analyses, consistent with reports of rightward asymmetry of the superior temporal sulcus/middle temporal gyrus in postmortem (Highley et al., 1999) and voxelwise reflection studies (Watkins et al., 2001). In addition, a rightward grey matter column map asymmetry was found superior to the planum temporale in the inferior frontal gyrus. White matter column map analysis revealed significant asymmetries that were in antiphase to the grey matter results in the perisylvian region (see Fig. 6). Significant asymmetries detected by the reflection and column map analyses presented here could arise due to local displacement of brain tissue, local volumetric differences, or a combination of the two. Fig. 6 illustrates this qualitatively. In particular, the larger left planum temporale appears to displace white matter immediately inferior and superior to the superior temporal lobe grey matter surface causing the characteristic antiphase asymmetry pattern revealed by the grey and white column map analyses. Deformation-based morphometry methods (e.g., Thirion et al., 2001) determine relative volume differences between the hemispheres without the confound of displacement. This method has previously been applied to the present cohort (Barrick, 2004) and revealed significant leftward asymmetry of the planum temporale and significant rightward asymmetry of the superior temporal sulcus/middle temporal gyrus (Barrick, 2004). These results suggest that the planum temporale and superior temporal sulcus/middle temporal gyrus findings are volumetric asymmetries whereas the remaining asymmetries in the perisylvian region may be due to structural displacements. Evidence that leftward planum temporale asymmetry is a volume rather than a shape change suggests that it is unlikely to be secondary to a mechanical shift of the hemispheres relative to each other. The displacements found by reflection and column map analyses may also be related to asymmetries in the trajectory and location of the superior temporal gyrus. Toga and Thompson (2003) reported an asymmetry in superior temporal gyrus morphometry such that the left superior temporal gyrus extends further posteriorly in the left hemisphere than the right, and that the right superior temporal gyrus is steeper toward the posterior of the brain than the left. A deformation-based surface morphometry technique has recently been reported (Chung et al., 2003), and application of this to investigate superior temporal lobe gyral thickness and cortical asymmetries will further improve our understanding of perisylvian morphology.

Quantification of cerebral asymmetry using the techniques described in the present study allowed investigation of the relationship between global torque and local planum temporale asymmetry, and the relationship between brain size and asymmetry. Crow (1997) postulates that a single underlying factor is responsible for brain asymmetry and brain size, and that an anomaly of brain asymmetry gives rise to schizophrenia. The strong correlations between torque and leftward planum temporale

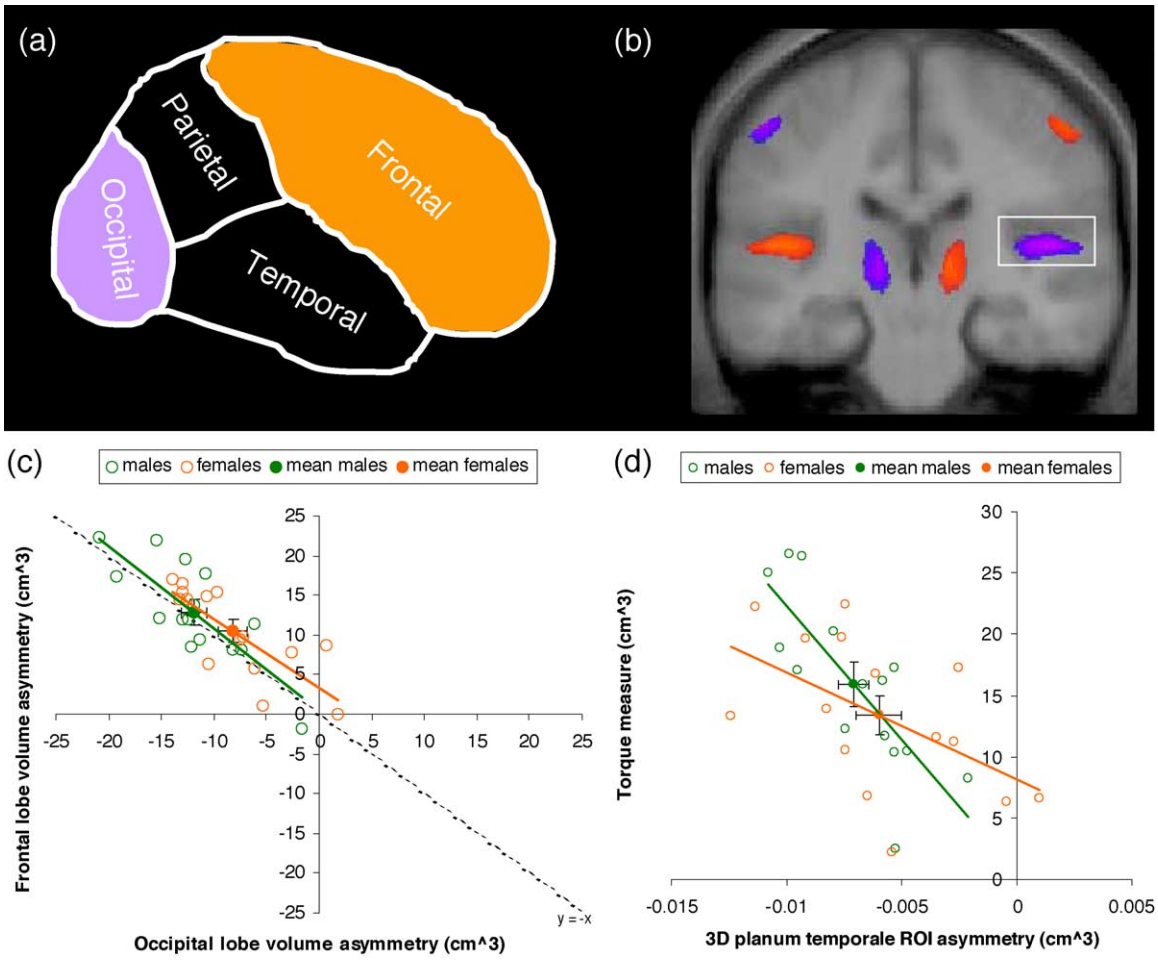

Fig. 5. Image (a) illustrates a schematic of the mask used to integrate lobe volumes from column map data. The relationship between frontal and occipital lobe asymmetry is shown in graph (c) for the male (green) and female (orange) subjects with lines of best fit and standard error bars marked. Image (b) illustrates the planum temporale ROI used for post hoc computation of planum temporale asymmetry from grey matter reflection asymmetry images. The relationship between planum temporale volume asymmetry and grey matter torque index is shown in graph (d) for the male (green) and female (orange) subjects with lines of best fit and standard error bars marked.

asymmetry and between the occipital and frontal components of torque reported here indicate that the most prominent components of cerebral asymmetry are related. We did not find evidence for a relationship between cerebral asymmetry and brain size, and conclude that the two are independent. This is in contrast to previous reports (Rosen, 1996) that greater asymmetry relates to reduced total volume. This assertion came from evidence that asymmetry is driven by one side possessing a smaller volume than is normal as opposed to one side possessing a greater volume than is normal (Rosen, 1996). Furthermore, we did not find a significant difference in brain torque between patients with schizophrenia and healthy controls in a previous application of the LowD technique (Mackay et al., 2003). Kennedy et al. (1999) reported that individuals with situs inversus totalis exhibit reversal of brain torque (along with reversal in asymmetry of all internal organs) but have normal incidence of right-handedness and of leftward language dominance. Taking these results together, it could be concluded that brain torque is a 'body asymmetry', that is, it relates to the asymmetry of the heart or other internal organs, but has no relevance for functional laterality. However, the presence of a significant relationship with planum temporale asymmetry suggests that brain torque is at least anatomically related to functionally relevant asymmetries. Future application of the techniques described here in combination with functional neuroimaging and neuropsychology paradigms will shed further light on the functional significance of structural asymmetry.

A criticism of voxel-based morphometry studies is that the technique is liable to a high false-positive rate (Ashburner and Friston, 2000), particularly if peak height thresholding is not employed. All results reported here were peak height thresholded and are frequently supported by evidence from region of interest quantification MRI or postmortem studies. For example, rightward parietal grey matter was detected by the reflection analysis. This asymmetry is in the region of the central sulcus and may relate to the reported leftward asymmetry of central sulcus depth found in male right-handers (Amunts et al., 2000). This could be further explored by extracting this region in left- and right-handed subjects as we have done for the planum temporale in the present study. Rightward asymmetries of the amygdala, hippocampus, and thalamus have been reported by several volumetric MRI studies (hippocampus: Jack et al., 1989; Mackay et al., 2000; amygdala and hippocampus: Szabo et al., 2001; thalamus: Watkins et al., 2001); however, leftward asymmetries of the amygdala and hippocampus have also been reported (Good et al., 2001). The

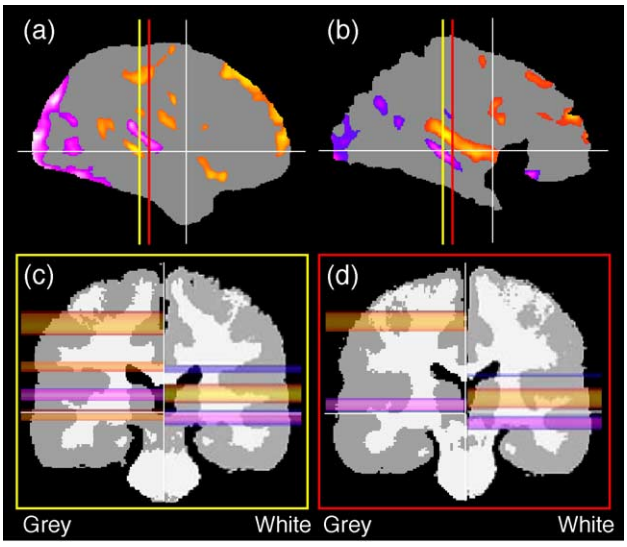

Fig. 6. Visual inspection of perisylvian asymmetry using column maps. Significant grey (a) and white (b) matter column map results are displayed above coronal slices through the perisylvian region in the anatomical locations indicated by the yellow and red lines overlain on images (a) and (b). Significant column map asymmetry results through the yellow and red coronal slices are overlain on mean grey and white matter binary segmentations computed across the 30 subjects in standard space (c and d). Significant grey and white matter column map results are shown overlain on the left and right hemispheres of the coronal images, respectively.

caudate nucleus was reported to be rightwardly asymmetric by Watkins et al. (2001), but leftwardly asymmetric by the present study and Good et al. (2001). Region of interest analyses have found the caudate nucleus to be rightwardly asymmetric (Ifthikharuddin et al., 2000; Raz et al., 1995), leftwardly asymmetric (Lacerda et al., 2003), and symmetric (Mackay et al., 1998), suggesting further analysis is needed to reliably determine left–right differences in this structure.

Compared to the large-scale studies of Watkins et al. (2001) and Good et al. (2001), the present study is exploratory as an investigation of sexual dimorphism in cerebral asymmetry. Nevertheless, the significant finding of increased rightward total matter hemispheric volume asymmetry in females compared to males is consistent with some postmortem reports (Skullerud, 1985; Von Bonin, 1962). In addition, the tendency for reduced leftward occipital asymmetry in females relative to males is consistent with results of previous torque studies (e.g., Amunts et al., 2000; Bear et al., 1986; Koff et al., 1986; Wada et al., 1975), and this may be the basis of the increased rightward asymmetry in females relative to males revealed by the cerebral hemisphere volume analysis. Interestingly, significantly greater rightward asymmetry was found in males relative to females for the white matter slice profile analysis in a region posterior to the corpus callosum. However, because this region was found by the slice profile analysis, the underlying white matter structures that contribute to this effect cannot be further localized in coronal slices. This region could be further investigated by quantitative analysis of reflection asymmetry images computed from Mean Diffusivity (MD) and Fractional Anisotropy (FA) maps (Pierpaoli and Basser, 1996) or by application of white matter fiber tractography techniques (Basser et al., 2000; Behrens et al., 2003) derived from Diffusion Tensor Images (DTI) in standard space (Jones et al., 2002) to determine shape or volume asymmetries in specific white matter structures.

Conclusion

We have reported the application of techniques for automatically quantifying global and local cerebral asymmetry, including the newly developed LowD column map, slice profile, and torque index analysis methods to a cohort of 30 right-handed healthy subjects. Brain torque and leftward planum temporale asymmetry were quantified, and a significant relationship was demonstrated between these measures of global and local asymmetry. Finally, LowD provides sufficient sensitivity to computation of asymmetry such that brain torque can be automatically quantified on a single-subject basis. This advance enables future experiments to investigate the relationship between torque and handedness, development, and functional lateralization in healthy subjects.

Acknowledgments

This research was funded by MRC grant G9900348. All images were displayed using mri3dX, http://www.aston.ac.uk/lhs/staff/singhkd/mri3dX/index.shtml.

References

Amunts, K., Jancke, L., Mohlberg, H., Steinmetz, H., Zilles, K., 2000. Interhemispheric asymmetry of the human motor cortex related to handedness and gender. Neuropsychologica 38, 304–312.

Aresu, M., 1914. La superficie cerebrale nell'vomo. Arch. Ital. Anat. Embriol. 12, 380–433.

Ashburner, J., Friston, K.J., 2000. Voxel-based morphometry—The methods. NeuroImage 11, 805–821.

Ashburner, J., Neelin, P., Collins, D.L., Evans, A., Friston, K., 1997. Incorporating prior knowledge into image registration. NeuroImage 6, 344–352.

Barrick, T.R., 2004. Automatic quantification of cerebral asymmetry. PhD thesis, University of Liverpool.

Barta, P.E., Pearlson, G.D., Brill, L.B., Royall, R., McGilchrist, I.K., Pulver, A.G., Powers, R.E., Casanova, M.F., Tien, A.Y., Frangou, S., Petty, R.G., 1997. Planum temporale asymmetry reversal in schizophrenia: replication and relationship to grey matter abnormalities. Am. J. Psychiatry 154 (5), 661–667.

Basser, P.J., Pajevic, S., Pierpaoli, C., Duda, J., Aldroubi, A., 2000. In vivo fiber tractography using DT-MRI data. Magn. Reson. Med. 44, 625–632.

Bastian, H.C., 1866. On the specific gravity of different parts of the human brain. J. Mental Sci. 56, 29.

Bear, D., Schiff, D., Saver, J., Greenberg, M., Freeman, R., 1986. Quantitative analysis of cerebral asymmetries. Fronto-occipital correlation, sexual dimorphism and association with handedness. Arch. Neurol. 43, 598–603.

Behrens, T.E., Johansen-Berg, H., Woolrich, M.W., Smith, S.M., Wheeler-Kingshott, C.A., Boulby, P.A., Barker, G.J., Sillery, E.L., Sheehen, K., Ciccarelli, O., Thompson, A.J., Brady, J.M., Matthews, P.E., 2003. Non-invasive mapping of connections between human thalamus and cortex using diffusion imaging. Nat. Neurosci. 6 (7), 750–757.

Bilder, R.M., Wu, H., Bogerts, B., Degreef, G., Ashtari, M., Alvir, J.M.J., Snyder, P.J., Lieberman, J.A., 1994. Absence of regional hemispheric volume asymmetries in first episode schizophrenia. Am. J. Psychiatry 151, 1437–1447.

Bilder, R.M., Wu, H., Bogerts, B., Ashtari, M., Robinson, D., Woerner, M., Lieberman, J.A., Degreef, G., 1999. Cerebral volume asymmetries in schizophrenia and mood disorders: a quantitative magnetic resonance imaging study. Int. J. Psychophysiol. 34, 197–205.

Blamire, A.M., Rowe, J.G., Styles, P., McDonald, B., 1999. Optimising imaging parameters for post mortem MR imaging of the human brain. Acta Radiol. 40 (6), 593–597.

Braune, C.W., 1891. Die Gewichtsverhältnisse der rechten zur linken Hirnhälfte beim Menschen. Arch. Anat. Physiol. 15, 253–270.

Broca, P., 1861. Remarques sur la siegé de la faculté du langue. Bull. Soc. Anat. Paris, Ser. 2 6, 330–357.

Chance, S.A., Esiri, M.M., Crow, T.J., 2004. Two components of brain asymmetry: volume torque reverses in schizophrenia but hemispheric shift ("petalia") is unchanged to appear in Schizophrenia Research.

Chui, H.D., Damasio, A.R., 1980. Human cerebral asymmetries evaluated by computerised tomography. J. Neurol., Neurosurg. Psychiatry 43, 873–878.

Chung, M.K., Worsley, K.J., Robbins, S., Paus, T., Taylor, J., Giedd, J.N., Rapoport, J.L., Evans, A.C., 2003. Deformation-based surface morphometry applied to grey matter deformation. NeuroImage 18, 198–213.

Crow, T.J., 1997. Schizophrenia as a failure of hemispheric dominance for language. Trends Neurosci. 20, 339–343.

Cunningham, D., 1892. Contribution to the Surface Anatomy of the Cerebral Hemispheres. Royal Irish Academy, Dublin.

Davidson, R.J., Hugdahl, K. (Eds.), Brain Asymmetry. MIT Press, Cambridge, MA.

Eberstaller, O., 1884. Zur oberflächenanatomie des grosshirnhemisphären. Wien. Med. Bl. 7, 479–482.

Elliot-Smith, G., 1907. New studies on the folding of the visual cortex and the significance of the occipital sulci in the human brain. J. Anat. Physiol. 16, 198–207.

Evans, A.C., Collins, D.L., Mills, S.R., Brown, E.D., Kelly, R.L., Peters, T.M., 1993. 3D statistical neuroanatomical models from 305 MRI volumes. Proceedings of IEEE-Nuclear Science Symposium and Medical Imaging Conference, Piscataway, New Jersey, pp. 1813–1817.

Falk, D., Hildebolt, C., Cheverud, J., Kohn, L.A., Figiel, G., Vannier, M., 1991. Human cortical asymmetries determined with 3D MR technology. J. Neurosci. Methods 39, 185–191.

Foundas, A.L., Leonard, C.M., Gilmore, R., Fennell, E., Heilman, K.M., 1994. Planum temporale asymmetry and language dominance. Neuropsychologica 32, 1225–1231.

Foundas, A.L., Faulhaber, J.R., Kulynych, J.J., Browning, C.A., Weinberger, D.R., 1999. Hemispheric and sex-linked differences in Sylvian fissure morphology: a quantitative approach using volumetric magnetic resonance imaging. Neuropsychiatry Neuropsychol. Behav. Neurol. 12, 1–10.

Friston, K.J., Ashburner, J., Frith, C.D., Poline, J.-B., Heather, J.D., Frackowiak, R.S.J., 1995. Spatial registration and normalization of images. Hum. Brain Mapp. 2, 165–189.

Garcia-Finana, M., Cruz-Orive, L.M., Mackay, C.E., Pakkenberg, B., Roberts, N., 2003. Comparison of MR imaging against physical sectioning to estimate the volume of human cerebral compartments. NeuroImage 18, 505–516.

Geschwind, N., Galaburda, A.M., 1985. Cerebral lateralization; biological mechanisms, associations and pathology: I. A hypothesis and a program for research. Arch. Neurol. 42, 428–459.

Geschwind, N., Levitsky, W., 1968. Human brain left–right asymmetries in temporal speech region. Science 161, 186–187.

Geschwind, N., Levitsky, W., 1991. Left–right asymmetry in temporal speech region. Biol. Psychiatry 29, 159–175.

Glicksohn, J., Myslobodsky, M.S., 1993. The relationship of patterns of structural brain asymmetry in normal individuals. Neuropsychologica 31 (2), 145–159.

Good, C.D., Johnsrude, I., Ashburner, J., Henson, R.N.A., Friston, K.J., Frackowiak, R.S.J., 2001. Cerebral asymmetry and the effects of sex and handedness on brain structure: a voxel-based morphometric analysis of 465 normal adult human brains. NeuroImage 14, 685–700.

Habib, M., Robichon, F., Lerier, O., Khalil, R., Salamon, G., 1995. Diverging asymmetries of temporo-parietal cortical areas: a reappraisal of Geschwind/Galaburda theory. Brain Lang. 48 (2), 238–258.

Highley, J.R., McDonald, B., Walker, M.A., Esiri, M.M., Crow, T.J., 1999. Schizophrenia and temporal lobe asymmetry. A post-mortem stereological study of tissue volume. Br. J. Psychiatry 175, 127–134.

Ifthikharuddin, S.F., Shrier, D.A., Numaguchi, Y., Tang, X., Ning, R., Shibata, D.K., Kurlan, R., 2000. MR volumetric analysis of the human basal ganglia: normative data. Acad. Radiol. 7, 627–634.

Jack Jr., C.R., Twomey, C.K., Zinsmeister, A.R., Sharbrough, F.W., Petersen, R.C., Cascino, G.D., 1989. Anterior temporal lobes and hippocampal formations: normative volumetric measurements from MR images in young adults. Radiology 172 (2), 549–554.

Jones, D.K., Griffin, L.D., Alexander, A.C., Catani, M., Horsfield, M.A., Howard, R., Williams, S.C.R., 2002. Spatial normalization and averaging of diffusion tensor MRI datasets. NeuroImage 17, 592–617.

Kennedy, D.N., O'Craven, K.M., Ticho, B.S., Goldstein, A.M., Makris, N., Henson, J.W., 1999. Structural and functional brain asymmetries in human situs inversus totalis. Neurology 53 (6), 1260–1265.

Kertesz, A., Black, S.E., Polk, M., Howell, J., 1986. Cerebral asymmetries on magnetic resonance imaging. Cortex 22 (1), 117–127.

Kertesz, A., Polk, M., Black, S.E., Howell, J., 1990. Sex, handedness, and the morphometry of cerebral asymmetries on magnetic resonance imaging. Brain Res. 530, 40–48.

Koff, E., Naeser, M.A., Pieniadz, J.M., Foundas, A.L., Levine, H.L., 1986. Computed tomographic scan hemispheric asymmetries in right- and left-handed male and female subjects. Arch. Neurol. 43 (5), 487–491.

Kulnych, J.J., Vladar, K., Jones, D.W., Weinberger, D.R., 1994. Gender differences in the normal lateralization of the supratemporal cortex: MRI surface-rendering mophometry of Heschl's gyrus and the planum temporale. Cereb. Cortex 4, 107–118.

Lacerda, A.L., Nicoletti, M.A., Brambilla, P., Sassi, R.B., Mallinger, A.G., Frank, E., Kupfer, D.J., Keshavan, M.S., Soares, J.C., 2003. Anatomical MRI study of basal ganglia in major depressive disorder. Psychiatry Res. 124, 129–140.

LeMay, M., 1976. Morphological cerebral asymmetries of modern man, fossil man and non-human primate. Ann. N. Y. Acad. Sci. 280, 349–369.

LeMay, M., 1977. Asymmetries of the skull and handedness. Phrenology revisited. J. Neurosci. 32, 243–253.

LeMay, M., Kido, D.K., 1978. Asymmetries of the cerebral hemispheres on computed tomograms. J. Comput. Assist. Tomogr. 2, 471–476.

Mackay, C.E., Roberts, N., Mayes, A., Downes, J.J., Foster, J., Mann, D., Edwards, R.H.T., 1998. An exploratory study of the relationship between face recognition memory and the volume of medial temporal lobe structures in healthy young males. Behav. Neurol. 11, 3–21.

Mackay, C.E., Webb, J.A., Eldridge, P.R., Chadwick, D.W., Whitehouse, G.H., Roberts, N., 2000. Quantitative magnetic resonance imaging in consecutive patients evaluated for surgical treatment of temporal lobe epilepsy. Magn. Reson. Imaging 18 (10), 1187–1199.

Mackay, C.E., Barrick, T.R., Roberts, N., DeLisi, L.E., Maes, F., Vandermeulen, D., Crow, T.J., 2003. Application of a new image analysis technique to the study of brain asymmetry in schizophrenia. Psychiatry Res. NeuroImaging 124 (1), 25–35.

Maes, F., Collignon, A., Vandermeulen, D., Marchal, G., Suetens, P., 1997. Multi-modality image registration by maximisation of mutual information. IEEE Trans. Med. Imaging 16 (2), 187–198.

Maes, F., Van Leemput, K., DeLisi, L., Vandermeulen, D., Suetens, P., 1999. Quantification of cerebral grey and white matter asymmetry from MRI, lecture notes in computer science. In: Taylor, C., Colchester, A. (Eds.), Proceedings 2nd International Conference on Medical Image Computing and Computer-Assisted Intervention—MICCAI'99, September 19–22, 1999, vol. 1679. Springer, Cambridge, UK pp. 348–357.

Miller, A.K., Alston, R.L., Corsellis, J.A., 1980. Variation with age in the volumes of grey and white matter in the cerebral hemispheres of man: measurements with an image analyser. Neuropathol. Appl. Neurobiol. 6 (2), 119–132.

Milner, B., 1971. Interhemispheric differences in the localization of psychological processes in man. Br. Med. Bull. 27 (3), 272–277.

Pfeiffer, R.A., 1936. Pathologie des horstrahlung und der corticaler. In: Bumke, F., Foerster, O. (Eds.), Handbuch der Neurologie. Springer, Berlin, pp. 523–626.

Pieniadz, J.M., Naeser, M.A., 1984. Computed tomographic scan cerebral asymmetries and morphologic brain asymmetries. Correlation in the same cases post mortem. Arch. Neurol. 41 (4), 403–409.

Pierpaoli, C., Basser, P.J., 1996. Toward quantitative assessment of diffusion anisotropy. Magn. Reson. Med. 36, 893–906.

Raz, N., Torres, I.J., Acker, J.D., 1995. Age, gender, and hemispheric differences in human striatum: a quantitative review and new data from in vivo MRI morphometry. Neurobiol. Learn Mem. 63, 133–142.

Rosen, G.D., 1996. Cellular, morphometric, ontogenetic and connectional substrates of anatomical asymmetry. Neurosci. Biobehav. Rev. 20 (4), 607–615.

Rubens, A.B., Mahowald, M.W., Hutton, J.T., 1976. Asymmetry of the lateral (Sylvian) fissures in man. Neurology 26, 620–624.

Rumsey, J.M., Dorwast, R., Verness, M., Denckla, M.B., Kruesi, J.P., Rapoport, J.L., 1986. Magnetic resonance imaging of the brain anatomy in severe developmental dyslexia. Arch. Neurol. 43, 1045–1046.

Skullerud, K., 1985. Variations in the size of the human brain. Influence of age, sex, body length, body mass index, alcoholism, Alzheimer changes, and cerebral atherosclerosis. Acta Neurol. Scand., Suppl. 102, 1–94.

Sled, J.G., Zijdenbos, A.P., Evans, A.C., 1998. A non-parametric method for automatic correction of intensity non-uniformity in MRI data. IEEE Trans. Med. Imaging 17 (1), 87–98.

Steinmetz, H., 1996. Structure, functional and cerebral asymmetry: in vivo morphometry of the planum temporale. Neurosci. Biobehav. Rev. 20 (4), 587–591.

Steinmetz, H., Galaburda, A.M., 1991. Planum temporale asymmetry: in vivo morphometry affords a new perspective for neuro-behavioural research. Read. Writ. 3, 331–343.

Steinmetz, H., Rademacher, J., Huang, Y., Hefter, H., Zilles, K., Thron, A., Freund, H.-J., 1989. Cerebral asymmetry: MR planimetry of the human planum temporale. J. Comput. Assist. Tomogr. 13 (6), 996–1005.

Szabo, C.A., Xiong, J., Lancaster, J.L., Rainey, L., Fox, P., 2001. Amygdala and hippocampal volumetry in control participants: differences regarding handedness. Am. J. Neuroradiol. 22 (7), 1342–1345.

Talairach, J., Tournoux, P., 1988. Coplanar Stereotactic Atlas of the Human Brain. Thieme Medical, New York.

Thirion, J.-P., 1998. Image matching as a diffusion process: an analogy with Maxwell's demons. Med. Image Anal. 2 (3), 243–260.

Thirion, J.-P., Prima, S., Subsol, G., Roberts, N., 2001. Automatic analysis of cerebral asymmetry. Med. Image Anal. 4, 111–121.

Toga, A.W., Thompson, P.M., 2003. Mapping brain asymmetry. Nat. Neurosci. 4, 37–48.

Van Leemput, K., Maes, F., Vandermeulen, D., Suetens, P., 1999a. Automated model-based tissue classification of MR images of the brain. IEEE Trans. Med. Imaging 18 (10), 897–908.

Van Leemput, K., Maes, F., Vandermeulen, D., Suetens, P., 1999b. Automated model-based bias field correction of MR images of the brain. IEEE Trans. Med. Imaging 18 (10), 885–896.

Von Bonin, G., 1962. Anatomical asymmetries of the cerebral hemispheres. In: Mountcastle, V.B. (Ed.), Interhemispheric Relations and Cerebral Dominance. Johns Hopkins Press, Baltimore, pp. 1–6.

Wada, J.A., Clarke, R., Hamm, A., 1975. Cerebral hemispheric asymmetry in humans. Cortical speech zones in 100 adults and 100 infant brains. Arch. Neurol. 32 (4), 239–246.

Watkins, K.E., Paus, T., Lerch, J.P., Zidjenbos, A., Collins, D.L., Neelin, P., Taylor, J., Worsley, K.J., Evans, A.C., 2001. Structural asymmetries in the human brain: a voxel-based statistical analysis of 142 MRI scans. Cereb. Cortex 11, 868–877.

Weil, A., 1929. Measurements of cerebral and cerebellar surfaces. Am. J. Physiol. Anthropol.

Weinberger, D.R., Luchins, D.J., Morihisa, J., Wyatt, R.J., 1982. Asymmetrical volumes of the right and left frontal and occipital regions of the human brain. Ann. Neurol. 11, 97–100.

Westbury, C.F., Zatorre, R.J., Evans, A.C., 1999. Quantifying variability in the planum temporale: a probability map. Cereb. Cortex 9 (4), 392–405.

Witelson, S.F., Kigar, D.L., 1992. Sylvian fissure morphology and asymmetry in men and women: bilateral differences in relation to handedness in men. J. Comput. Neurol. 323, 326–340.

Worsley, K.J., Marret, S., Neelin, P., Vandal, A.C., Friston, K.J., Evans, A.C., 1996. A unified statistical approach for determining significant voxels in images of cerebral activation. Hum. Brain Mapp. 4, 58–73.

Zhang, Y., Brady, M., Smith, S., 2001. Segmentation of brain MR images through a hidden Markov random field model and the expectation-maximisation algorithm. IEEE Trans. Med. Imaging 20 (1), 45–57.

Zijdenbos, A.P., Forghani, R., Evans, A.C., 1998. Automatic quantification of MS lesions in 3D MRI brain data sets: validation of INSECT. Medical Image Computing and Computer-Assisted Intervention (MICCAI'98), pp. 439–448.

Zilles, K., Dabringhaus, A., Geyer, S., Amunts, K., Qu, M., Schleicher, A., et al., 1996. Structural asymmetries of the human forebrain and the forebrain of non-human primates and rats. Neurosci. Biobehav. Rev. 21, 593–605.